# Miniature holistic displacement sensor by immersion diffractive interferometry

Yves Jourlin, O. Parriaux, J. Fuchs

# Miniature holistic displacement sensor by immersion diffractive interferometry

**Yves Jourlin[1,*], Olivier Parriaux[1] and Jörg Fuchs[2]**

[1]*Laboratoire Hubert Curien, UMR CNRS 5516, Université Jean Monnet, 18 rue Prof. Benoit Lauras, 42000 Saint-Etienne, France*

[2]*IAP, Friedrich-Schiller-Universität, Jena ,Germany*

*corresponding author: yves.jourlin@univ-st-etienne.fr

**Abstract:** High interference contrast is obtained in a miniature dual-grating transmission displacement sensor submitted to an essentially uniform light flood of arbitrary polarization with multifunctional liquid film between gratings.



**OCIS codes:** (050.1950) Diffraction gratings; (120.3180) Interferometry; (220.4830) Systems design

## References and links

1. M. Nevière, E. Popov, B. Bojhkov, L. Tsonev, and S. Tonchev, "High-Accuracy Translation-Rotation Encoder with Two Gratings in a Littrow Mount," Appl. Opt. **38**, 67-76 (1999).
2. A. Spies, "Linear and angular encoders for the high-resolution range," in *Proceeding of Progress in Precision Engineering and Nanotechnology*, (Braunschweig, Germany, 1997), pp. 54–57.
3. O. Parriaux, Y. Jourlin, J. Jay, Y. Alayli, F. Lozes, and J. L. Noullet, "Long Range, nanometer resolution microoptical sensor," In *Proceeding of the 1st International Conference and general meeting of the European Society for Precision Engineering and Nanotechnology* (Bremen, Germany, 1999), pp. 264-270.
4. Y. Jourlin, J. Jay, and O. Parriaux, "Compact diffractive interferometric displacement sensor in reflection," Prec. Eng. **26**, 1-6 (2002).
5. P. Arguel, J. Valentin, S.Fourment, F. Lozes-Dupuy, G. Sarrabayrouse, S. Bonnefont, Y. Jourlin, S. Reynaud, N. Destouches, A.V. Tishchenko, and J. Jay, "A monolithic optical phase-shift detector on silicon," Sensors J. **5**, 1305-1309 (2005).
6. A. Teimel, "Technology and applications of grating interferometers in high-precision measurement," Prec. Eng. **14**, 147-154 (1992).
7. S. Tsuda, T. Takahama, and Y. Hishikawa, H. Tarui, H. Nishiwaki, K. Wakisaka, S. Nakano, "a-Si technologies for high efficiency solar cells," J. Non-Cryst. Solids **164-166**, 679-684 (1993).
8. G. Voirin, U. Benner, F. Clube, Y. Darbellay, O. Parriaux, S. Schneider, and P. Sixt, "Performance of interferometric rotation encoder using diffraction gratings," Proc. SPIE **3099**, 166-175 (1997).
9. N. Lyndin. "MC Grating Software Development Company," http://www.mcgrating.com/ (dec.2008)
10. J. Thiel and E. Spanner, "Interferential linear encoder with 270 mm measurement length for nanometrology," In *Proceeding of the 1st International Conference and general meeting of the European Society for Precision Engineering and Nanotechnology* (Bremen, Germany, 1999), pp. 419-422.

## 1. Introduction

High resolution translation and rotation encoders using diffractive interferometry are usually composed of a first grating (the grating scale or the encoder disk) of wavelength scale period which diffracts an incident beam into at least two diffraction orders, and a second, smaller grating (the readout grating) which projects the said diffraction orders into common directions Thes two beams interfere and deliver optical power signals which are sinusoidal functions of the phase shift between the recombined order due to the relative displacement of the two gratings [1, 2, 3, 4]. The angularly separated interfered beams are left to propagate until they are spatially separated to permit the individual photodection of their modulated optical power. A photodetector placed close to the readout grating in the interferogram before the interfered beams have walked off would essentially detect a DC signal for a reason of conservation of energy [5]. This represents a limit to miniaturization. There is today a strong need in domains such as microsystems, micromotors to use a diffractive interferometric scheme in order to obtain very high resolution in translation and rotation sensing despite the small size of the

#107444 - $15.00 USD Received 11 Feb 2009; revised 26 Mar 2009; accepted 28 Mar 2009; published 15 May 2009

grating encoder. In such application domains there is no space available to separate the interfered beams before detection; besides, the incident beam cross-section is larger than the full encoder scale or disk whereas in state of the art encoders the beam cross-section is notably smaller than the encoder grating. This places new constraints in the design of optical measurement systems and calls for novel schemes to retrieve the phase shift created by the relative displacement between two miniature gratings. The present paper brings one possible solution whereby a photodetector placed immediately behind the readout grating receives an optical power signal of high contrast.

## 2. Principle of a high contrast holistic scheme

The proposed grating interference scheme comprises two identical transmission gratings of wavelength scale period $\Lambda$ as depicted in Fig. 1. This is a known scheme [6] where the normally incident beam at wavelength $\lambda$ is split into the $-1^{st}$ and $+1^{st}$ orders $B_{+1}$ and $B_{-1}$ under the diffracted angle $\theta_d = \sin^{-1}(\lambda/\Lambda)$ in air with minimum transmission in the $0^{th}$ order. The diffracted beams get diffracted back onto the $0^{th}$ transmitted order in the substrate of the second grating with a large field overlap if the two gratings are close to each other. There is also an interference in the directions of the $1^{st}$ diffraction orders in the said substrate where there is a superposition of the $0^{th}$ transmitted order of $B_{+1}$ and the $-2^{nd}$ order of $B_{-1}$, and conversely.

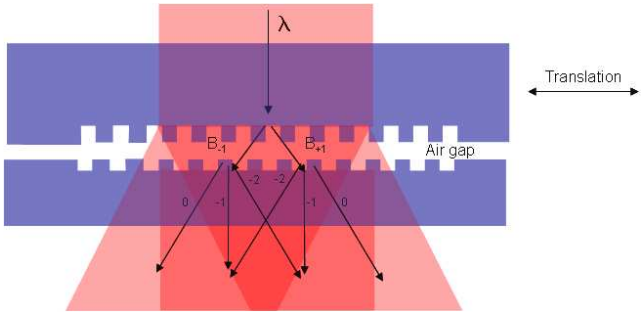


Fig. 1. Standard diffractive interferometric sensor scheme with overlap of interfered orders and contrast cancellation.

High diffraction efficiency can be obtained with a binary corrugation fabricated by etching or embossing of the substrate made of glass or fused silica or polymer. The optical power propagated in the three interference directions comprises generally a DC and an AC component which can be detected at the back side of the substrate of the second grating or further downstream after spatial separation of the three beams. If for sake of miniaturization a detector is placed close to the second grating, all three power signals will be detected at once with an almost complete cancellation of the AC component because of energy conservation. The law of conservation of energy actually concerns all propagating orders diffracted by the second grating, transmitted as well as reflected orders, it does not concern the transmitted orders only. However, the energy redistribution between reflected and transmitted orders upon a relative displacement between the gratings is very small in gratings of weak index contrast such as a simple corrugation at the substrate surface. This implies that the total power diffracted into the substrate is almost conserved upon displacement, thus the total AC power is close to constant. Therefore, the power modulation into the normal direction is almost compensated by the AC power components along the two oblique directions. This is a major difficulty in the use of diffractive interferometry in small systems and microsystems.

One solution to prevent interference contrast cancellation is to redirect the oblique beams so that they do not reach the detector. The rationale of the solution is illustrated in Fig. 2.

#107444 - $15.00 USD Received 11 Feb 2009; revised 26 Mar 2009; accepted 28 Mar 2009; published 15 May 2009

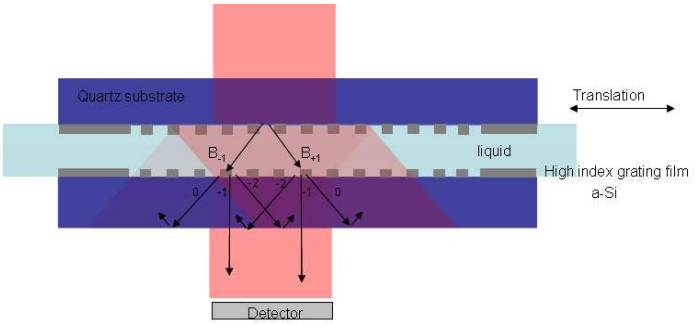


Fig. 2. Angular filtering of contrast canceling orders by diffraction in a fluid and a total internal reflection transmission scheme.

This can be made by forbidding the oblique beams from exiting the second grating substrate by total internal reflection. However, this is impossible by the very fact that the beams $B_{+1}$ and $B_{-1}$ do propagate in the air gap between gratings. The solution is to fill the gap with a liquid of refractive index n and to adjust the grating period so that the diffraction orders $B_{+1}$ and $B_{-1}$ have a horizontal component of their k-vector $nk_0\sin\theta_d$ larger than the k-vector $k_0 = 2\pi/\lambda$ of a plane wave in air, in other words, so that the grating K-vector $K_g = 2\pi/\Lambda$ is larger than $k_0$. In so doing, the interference products along the oblique beams in the second grating substrate get totally reflected at the basis of the latter and trapped in it. Using a liquid between two translating or rotating parts in microsystems or micromotors is not as awkward as it would be in larger size encoders. A liquid may have other functions like for instance that of keeping a good concentricity and a stable spacing between two very small grating encoder disks by surface tension or the function of a lubricant between the two rotating parts in close proximity. However, using a liquid between two transmission corrugation gratings tends to cancel the index contrast between the corrugated substrate and the external medium: this decreases the diffraction efficiency or requires a groove depth that is impossible to fabricate. The solution that was found is to make the corrugation in a material of very high refractive index which can easily be deposited onto a low cost substrate material. Such is amorphous silicon (a-Si), either deposited by evaporation or CVD, the latter being widely known and used in solar cells, and can be a very low cost technology [7]. Highly hydrogenated amorphous silicon has low losses down to the red, therefore it can be used as the corrugated film with low price light sources in the red and near IR spectrum where single crystal silicon detectors can still be used. Different materials are also possible which require not too large a corrugation depth: most high index metal oxides such as $TiO_2$, $ZrO_2$, $HfO_2$, $Ta_2O_5$, $Nb_2O_5$, $Si_3N_4$, iron oxide [8]. A preferred layer material is however amorphous silicon with its very large index and since it is in principle easily etchable by RIE.

The above described device permitting the holistic measurement of a miniature displacement sensor faces one inherent problem which is that of the generation of a second interfered signal in quadrature with a first interfered signal. The fact that one detects the modulation of a light beam over its full cross-section forbids the standard solution used in conventional rotation sensors whereby a second beam measures the signal of a phaseshifted second grating track. A solution which would preserve the holistic character of the measurement is polarization diversity: in the example of a rotation micro-sensor, there would be between the light source and the double-grating sensor of Fig. 2 a monolithic polarizing element simply patterned in the form of one inner circular polarizing zone that transmits one linear polarization to one sensor grating track and one outer circular polarizing zone transmitting the orthogonal linear polarization to the phaseshifted sensor grating track. The interfered transmitted beam passes then through a polarizing beam splitter and two identical, non-segmented photodetectors detect holistically the interfered signal of each grating track and thus deliver the sine and cosine power signals resulting from the relative rotation of the gratings of Fig. 2. This polarization diversity scheme will not be demonstrated in the present

#107444 - $15.00 USD Received 11 Feb 2009; revised 26 Mar 2009; accepted 28 Mar 2009; published 15 May 2009

paper which is essentially concerned with the demonstration of holistic measurement of the relative rotation between two single tracks.

### 3. a-Si grating design and fabrication

We made the proof of principle of the described solution in a miniature rotation encoder implementation in order to demonstrate practically that diffractive interferometry can achieve very high resolution even with an encoder disk of diameter as small as 0.5 mm. The chosen wavelength was that of a VCSEL at 890 nm to also permit a functional test with a standard LED or low cost VCSELs often used in encoders. Although the described grating interference scheme is essentially achromatic, a laser source is recommended since the incident beam must have a high spatial coherence to prevent interference contrast fading due to imbalance between optical paths. A grating period of 800 nm was chosen which implies that the $+1^{st}$ and $-1^{st}$ diffraction orders in air are cut off. With a water or oil film between the two gratings the direction of the beams $B_{+1}$ and $B_{-1}$ is 52 degrees relative to the normal whereas the critical angle between water and air is 48 degrees. A radial grating diameter of 521 µm was chosen to provide 2048 geometrical periods in a circle, i.e., 4096 electrical periods in the detected interference signal. One critical experimental difficulty with such small grating track diameter is that the least eccentricity between the two radial gratings will cause a misalignment between the grating lines. An overlap of the lines of the two gratings leads to a fall of the interference contrast since the single detector collecting the whole flux crossing both gratings will detect a complex interferogram with a DC average of the varying interference fringes. It was estimated that the maximal length of the radial grating lines, i.e. the maximum width of the grating track of 521 µm diameter is 25 µm for a maximum tolerated eccentricity of 2 µm. This places tough specifications on the experimental mechanical bench. The linear period is 0.8µm which also corresponds to an angular period close to 3 mrad. Fig. 3(a) is the cross-section of the encoder disk along a diameter showing the a-Si – chromium bilayer and the centering circle and grating ring trenches. Fig. 3(b) is the top view of the same with some radial grating periods in the insert; the centering ring has a 200 µm diameter, 5 µm width and the grating ring has a 521 µm diameter and 25 µm width.

.

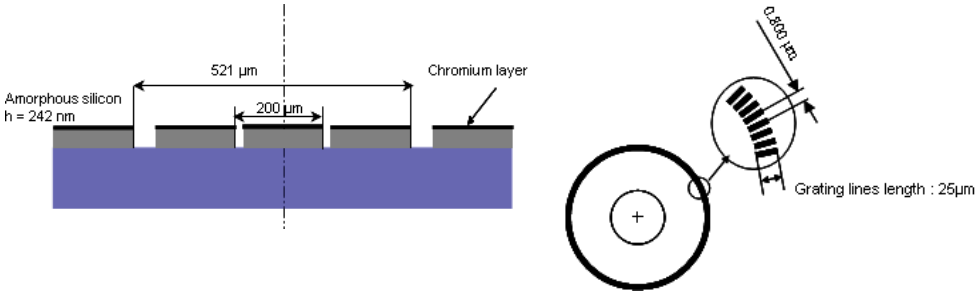


Fig. 3. Cross section of the substrate along a diameter (a) and top-view of the grating ring design with some grating periods in the insert (b).

Figure 4 represents the pictures of the fabricated grating disk taken by an optical microscope, Fig. 4(a) and the SEM scan of a number of periods of the radial grating, Fig. 4(b).

#107444 - $15.00 USD Received 11 Feb 2009; revised 26 Mar 2009; accepted 28 Mar 2009; published 15 May 2009

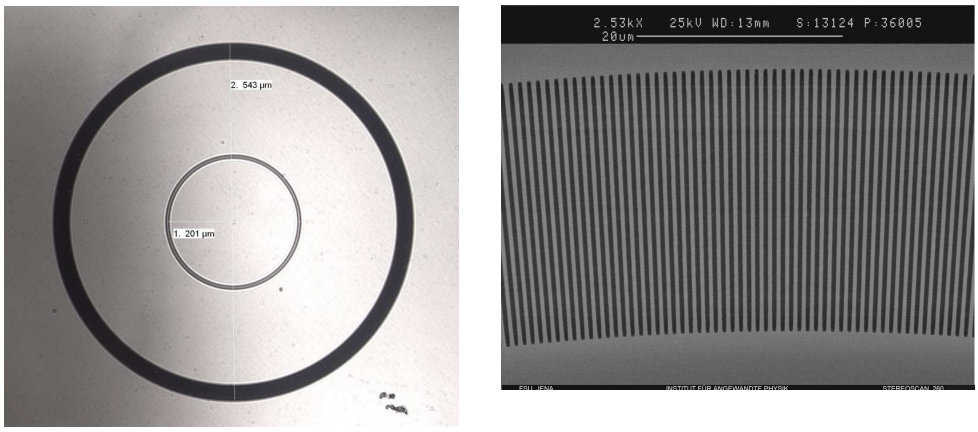


(a) (b)

Fig. 4. Optical microscope *picture (X100) of the complete structure* (a) and SEM scan pictures of the etched amorphous silicon grating ring (b).

The corrugation is binary in the form of rectangular grooves all through the amorphous silicon layer of refractive index assumed to be 3.6 on a substrate of fused silica. An optimisation code based on the true mode method [9] searches for the groove depth and line/period duty cycle giving the maximum $+1^{st}$ and $-1^{st}$ diffraction efficiency and minimum $0^{th}$ order transmission in the presence of an oil cover with refractive index of 1.6, for both TE and TM incident polarizations since the device must not place any restrictive requirement on the light source. Fig. 5(a) is the cross-section of the modelled polarization independent transmission grating. The optimized structure is characterized be a 358 nm line width and 442 nm space width for 242 nm a-silicon layer thickness. The structure gives theoretically 42% diffraction efficiency for the TE polarization with 4% residual 0th transmitted order and 33% for the TM polarization and 8% residual 0th order transmission as illustrated in Fig. 5(b). Note that the TE polarization is defined with the electric field parallel to the grating lines.

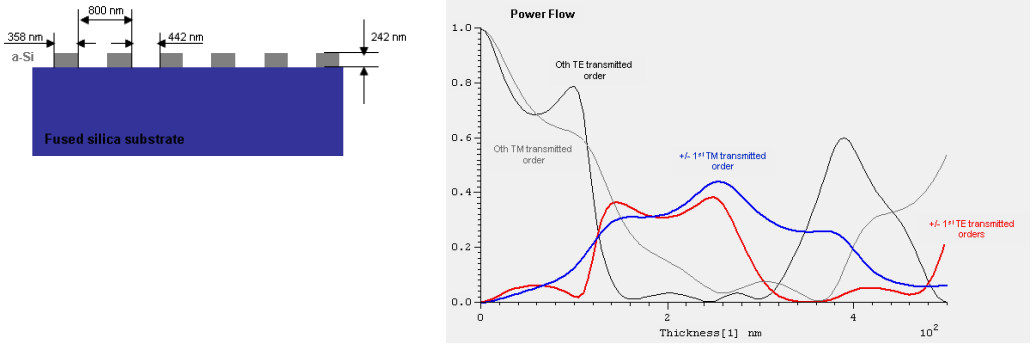


(a) (b)

Fig 5. Cross section of the optimized structure (a) and efficiency spectra for the $0^{th}$ and +/- $1^{st}$ transmitted orders of the TM and TE polarizations versus grating thickness (b).

A number of radial gratings were written in an e-beam resist layer by means of an electron beam pattern generator from FSU of Jena (Vistec SB350 OS). A thin chromium layer of 30 nm thickness was deposited on the amorphous silicon layer beforehand. The first etching trials were made on an a-Si layer deposited by the CVD used for amorphous silicon solar cells. These were not successful because the surface of such a-Si layer is not flat enough at the

#107444 - $15.00 USD Received 11 Feb 2009; revised 26 Mar 2009; accepted 28 Mar 2009; published 15 May 2009

submicrometer scale to permit a uniform microstructuring. It was decided to resort to evaporated silicon layers which turned out to lead to a smoother surface topology with the penalty of larger losses; however, the silicon layer is so thin that the optical function of the grating is practically unaffected. The chromium layer was etched by means of a chlorine plasma, and the silicon grooves by RIBE. Fig. 6 are the TSEM scan of some silicon grating grooves performed on an ultra-thin slice cut by focused ion beam transversally to the lines. One sees that the grooves are not completely open through the silicon layer and that the duty cycle is close to the desired 44.7 %. This discrepancy is not likely to perturb the overall optical function. The effect is a drop of the diffraction efficiency and a more pronounced polarization dependence.

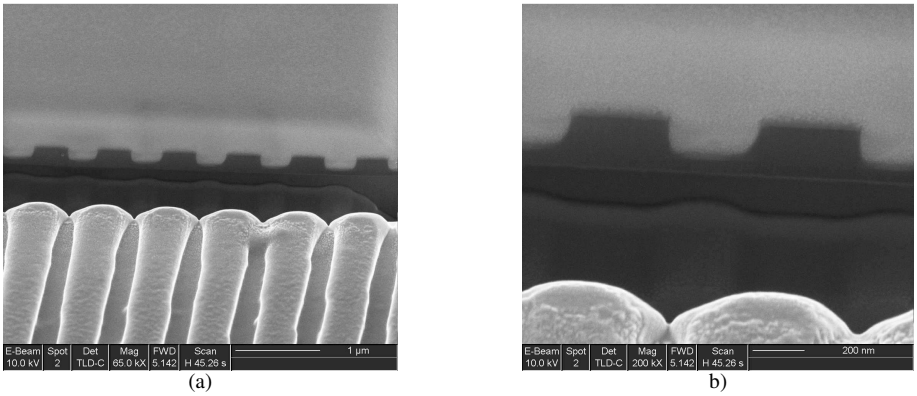


(a) b)

Fig. 6. TSEM pictures of the amorphous silicon corrugation with different magnification (a) x 65.000 , (b) x 200.000.

The last fabrication operation is the selective removal of the chromium layer. As the incident beam illuminates an area which is larger than the complete grating device, and that a very small area only of the incident beam gives rise to a modulation of the transmission upon relative rotation between gratings (the grating ring area is about $5.10^{-2}$ $mm^2$ only), the AC/DC contrast would be hardly measurable. This is why the chromium layer is left all over the surface except in the grating ring. The selective removal of the chromium layer is made by depositing a photoresist layer all over the sample at the chromium side, then exposing it to a UV lamp from the back side through the etched silicon grating. After the resist development, a chrometch removes the chromium that was left on the silicon lines and leaves it unetched everywhere else.

## 4. Experimental evidence of high contrast modulation

A mechanical bench (Fig. 7) was designed and built to permit the concentricity adjustment and also the relative rotation of the two radial gratings with a prescribed spacing between them filled with liquid (oil or water).

As shown in Fig. 7, the experimental set up consists of two high precision XYZ stages which hold the two grating ring substrates. One of the grating ring substrates is mounted on another XY stage and rotation stage in order to align the grating ring centre on the rotation axis. The experimental bench enables to perform the alignment of the two 500 µm diameter rings within a few micrometers.

#107444 - $15.00 USD Received 11 Feb 2009; revised 26 Mar 2009; accepted 28 Mar 2009; published 15 May 2009

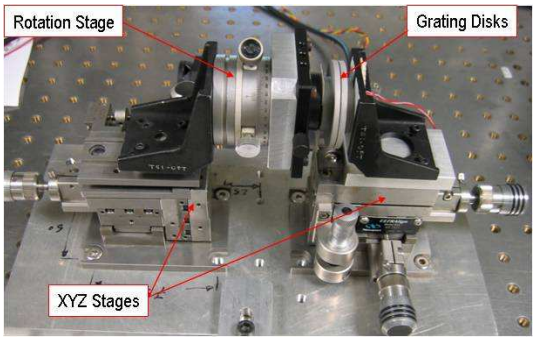


Fig. 7. Picture of the experimental bench with the two XYZ stages and the rotation stage.

The first step is the adjustment of the concentricity of the grating ring mounted on the rotation stage. The second step is the alignment of the two grating rings. The alignment is made with the help of an additional camera. Fig. 8 shows the two grating rings and centering circles acquired by the camera during the alignment phase.

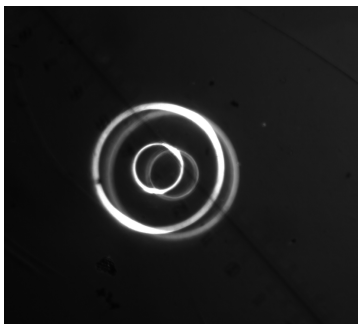

Fig. 8. Picture of the grating rings acquired by the camera during the alignment step.

The source and the detector were aligned relative to the rotation axis. The source used is a low cost VCSEL emitting at 850 nm with 2.5 mW power and the detector is a silicon based photodiode. The liquid used between the two gratings in this case is a transparent oil of refractive index 1.55. The signal picked up by the detector upon relative rotation shown in Fig. 9 demonstrates that a definite modulation takes place upon the displacement. The corresponding signal period is half the period of the grating, i.e., 0.4µm as expected. The modulation depth (AC/DC) is quite small, close to 5%. This is due to the non-zeroth transmission of the chromium film outside the grating ring which increases the DC component; as the area of the grating ring (about 0.05 mm²) is much smaller than the area illuminated by the laser on the photodiode (5 mm²), the transmission of the uniform chromium/silicon bilayer being 12%, one can not expect actually more than 8% contrast. Taking into account the high DC background of the chromium layer transmission, the measured 5% contrast modulation is not far from the expectable 80-90% considering the light traversing the rings only. The way to a larger contrast is simply to make the chromium layer thicker and also to better adapt the detector size to the diameter of the grating rings.

#107444 - $15.00 USD Received 11 Feb 2009; revised 26 Mar 2009; accepted 28 Mar 2009; published 15 May 2009

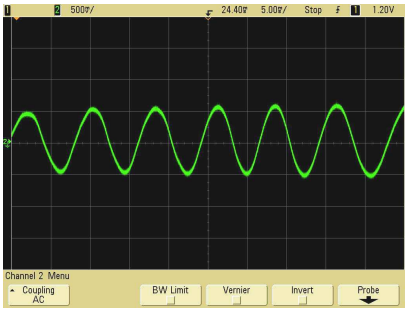


Fig. 9. Detected signal upon relative rotation.

## 5. A reflection variation

The same rationale scheme can be applied to a reflection scheme as represented in Fig. 10. The basis configuration is known [10]. The incident beam experiences a first diffraction event (the splitting) at the first transmission grating, both diffracted orders get reflected by the second reflection grating of double spatial frequency under the $-1^{st}$ order Littrow condition in the liquid film, then experience a second diffraction event (the mixing) at the first grating. This scheme of the state of the art leads to a quite cumbersome hardware which does not lend itself to miniaturization. Detecting all orders by means of a single detector placed close to the splitting/mixing grating would similarly lead to a cancellation of the interference contrast.

As demonstrated in Fig. 10, the presence of the liquid permits to forbid the oblique beams from exiting the top substrate into the air. Therefore the sole interference direction is the normal along which a high interference contrast is obtained. The advantage of such scheme is that not only it is essentially achromatic, but it does not place any demand on the spatial coherence of the source, consequently a LED can be used. Its drawback is the necessity of a beam splitter. In the device of the state of the art, non-degenerate functions of the phase shift between the two gratings in relative displacement are obtained by detecting the oblique beams which are now trapped in the top substrate. However, sine and cosine functions can also be obtained by placing two gratings side by side on the same substrate with the adequate offset between them.

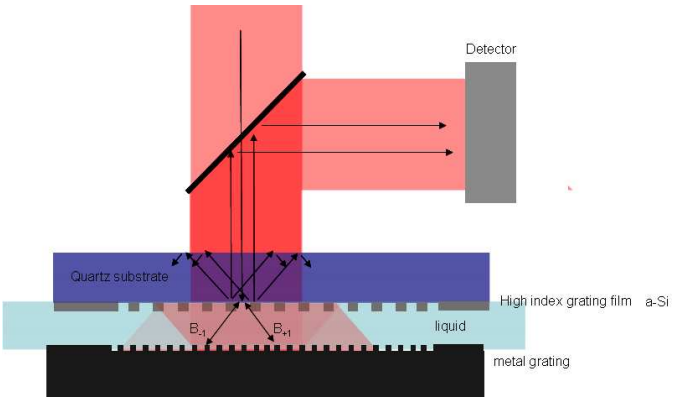


Fig. 10. Angular filtering of contrast canceling orders by diffraction in a fluid and total internal reflection.

#107444 - $15.00 USD Received 11 Feb 2009; revised 26 Mar 2009; accepted 28 Mar 2009; published 15 May 2009

## 6. Conclusion

The principle of diffractive interferometry is shown to be applicable to microsensors without loss of interference contrast and thus to permit high resolution despite the small size of the encoder. This has been achieved by introducing a possibly multifunctional liquid film between gratings which allows to angularly filter out contrast cancelling interference products, and by resorting to a very interesting high index optical material which can be advantageously used in the visible range: amorphous silicon.
The concept has been demonstrated in the case of a miniature rotation sensor of less than 1 mm diameter uniformly submitted to a flood of light. A reflection scheme exhibiting achromaticity as well as spatial coherence tolerance is proposed.

## Acknowledgment

The authors are grateful to David Troadec, IEMN, Lille, for the TEM analysis of a FIB-sliced silicon grating. The authors are also grateful to Dr. Svetlen Tonchev for his assistance in the inventive lithographic step of chromium removal from the grating track.

#107444 - $15.00 USD Received 11 Feb 2009; revised 26 Mar 2009; accepted 28 Mar 2009; published 15 May 2009